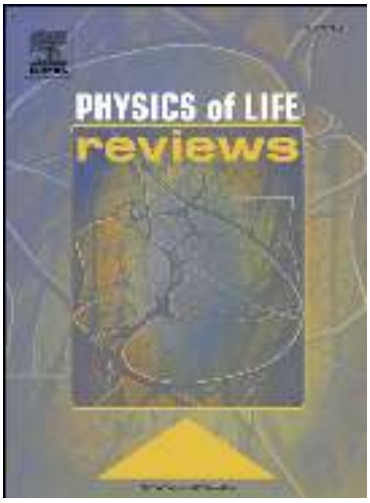

The growth of cognition: free energy minimization and the embryogenesis of cortical computation

J.J. Wright, P.D. Bourke

PII: S1571-0645(20)30015-4
DOI: https://doi.org/10.1016/j.plrev.2020.05.004
Reference: PLREV 1199

To appear in: *Physics of Life Reviews*

Received date: 28 May 2020
Accepted date: 29 May 2020

Please cite this article as: Wright JJ, Bourke PD. The growth of cognition: free energy minimization and the embryogenesis of cortical computation. *Phys Life Rev* (2020), doi: https://doi.org/10.1016/j.plrev.2020.05.004.

Highlights

- The free energy principle is applied to embryogenesis of the cortex.
- Developing neurons are selected to maximize pulse synchrony.
- Realistic cortical anatomy emerges for a wide-range of structures.
- Learning obeys Friston's "self-evidencing" with minimum free energy and bounded entropy.
- Computational properties accord with Perlovsky's "dynamic logic".

The growth of cognition: free energy minimization and the embryogenesis of cortical computation.

J. J. Wright
Centre for Brain Research, and Department of Psychological Medicine, School of Medicine, University of Auckland, Auckland, New Zealand.
jj.w@xtra.co.nz

P.D. Bourke
School of Social Sciences, Faculty of Arts, Business, Law and Education, University of Western Australia, Perth, Australia.
paul.bourke@uwa.edu.au

Abstract

The assumption that during cortical embryogenesis neurons and synaptic connections are selected to form an ensemble maximising synchronous oscillation explains mesoscopic cortical development, and a mechanism for cortical information processing is implied by consistency with the Free Energy Principle and Dynamic Logic.A heteroclinic network emerges, with stable and unstable fixed points of oscillation corresponding to activity in symmetrically connected, versus asymmetrically connected, sets of neurons. Simulations of growth explain a wide range of anatomical observations for columnar and non-columnar cortex, superficial patch connections, and the organization and dynamic interactions of neurone response properties. An antenatal scaffold is created, upon which postnatal learning can establish continuously ordered neuronal representations, permitting matching of co-synchronous fields in multiple cortical areas to solve optimization problems as in Dynamic Logic. Fast synaptic competition partitions equilibria, minimizing "the curse of dimensionality", while perturbations between imperfectly partitioned synchronous fields, under internal reinforcement, enable the cortex to become adaptively self-directed. As learning progresses variational free energy is minimized and entropy bounded.

Key Words : free energy principle, cortical embryogenesis, synchronous oscillation, neuronal representation, dynamic logic, physics of the mind.

1. Introduction

1.1 The free energy principle and computation in the brain

Determination of elementary laws for the organization of the brain, and its means for representation and manipulation of information, are two major, and related, scientific goals [1,2,3,4,5].

Toward the first of these goals, Friston and colleagues [6,7,8,9,10,11], in their "Free Energy Principle", have extended the work of Jaynes [12], emphasising mathematical unity from the physical principle of least action, through thermodynamics, and, via considerations of optimum information representation, to living systems and to machine and real intelligence. By separating evolving systems into hierarchies of subsystems, each defined by enclosure in a Markov blanket – that is, a means of receiving inputs from, and generating outputs to, the surround - each subsystem's dynamics can then be described in analogy to thermodynamic minimization of free

energy – and in the case of living systems, with the increase of entropy bounded. Consequently, since representation of meaningful information in noisy data requires optimum minimization of model complexity [13], the brain's self-organisation during learning involves a gradient flow on a functional that entails a minimisation of complexity [14] - with complexity, measured by the degrees of freedom that are used to provide an accurate representation of sensory input, diminishing as learning progresses, minimizing discrepancy between Bayesian prior and posterior representations of the causes of sensory perturbations. Thus the brain operates to minimize surprisal – having learnt to maintain its survival by forming a sensory-motor model of its relations with the environment - and surprisal is the informational analogue of thermodynamic free energy. The principle offers strong theoretical assurance of the globality of the learning - a property referred to by Friston as"self-evidencing" - but does not necessarily specify the variables that undergo dimension reduction during learning, and has not yet been translated into specific cellular anatomical and physiological terms.

Toward the second goal, Perlovsky and colleagues' "Physics of the Mind" [15,16,17,18,19,20,21,22] aims to specify a psychologically realistic information processing mechanism for the brain, which bypasses bottle-necks of standard computation. In artificial neural network (ANN) simulations, their "Dynamic Logic" entails the emergence of disentangled and orthogonalized solutions to a type of optimization whereby "vague" (ie, less orthogonalized) neural representations at lower and higher levels of the neural hierarchy are rapidly matched to achieve "crisp" neural representations, forming a basis for the continuous interaction of sensory inputs, perceptual, and intentional processes. Generalisation to interactions between many cortical areas implies a mechanism for overall brain coordination. Although less abstract, this account, too, lacks specification in cellular biological terms, but does direct attention toward pulse dynamics and synchrony.

Crucially, dynamic logic may be regarded as a special case of the free energy principle, and offers detail for the required mechanisms for general associative learning required to fill out the application of the free energy principle to brain function. In both concepts, minimization of variational free energy is equivalent to restriction of the degrees of freedom of the system dynamics; ie, the emergence of generalised synchronisation on relatively low dimensional manifolds that preserve mutual information between neuronal dynamics, and the sensorium [23], and among cortical areas. This suggests that action potential synchronization, discovered by Singer and colleagues [24,25,26,27,28], might mediate the brain's development and learning – and in turn suggests a strong test for the applicability of the free energy principle. If the principle is valid in this context, then simulations of the emergence of synchrony during neurodevelopment and later learning ought to result in outcomes with realistic micro and mesoscopic neuroanatomy, just as, at a basic physical level, application of the principle of least action prescribes the parabolic trajectory of a projectile. It might be further hoped that a cellular basis for dynamic logic would incidentally become apparent. Our work, although separately motivated by the problems described in the following sections, has addressed both aspects. We hope to show in this paper that the cellular mechanisms required for both the self-evidencing learning of the free energy principle, and the powerful associative learning of dynamic logic, follow from our account of cortical dynamics and embryogenesis.

1.2 The mesoscopic scale of cortical organisation

During embryogenesis cortical neuron precursors divide and migrate [29,30,31,32,33]. Developing neurons become progressively elongated, synapses connect neurons one-to-many, in a sparse fashion, with few synapses formed for the number of contacts made between axons and dendrites [33,34]. A network with low degrees of separation and weak cell-to-cell connectivity is created, subject to synaptic learning rules [35], competition for critical substrates [36] and the apoptotic death [37,38,39] of many cells. Apoptosis is attributed to competition for neurotrophic growth factors, and a caspase "execution" pathway. For our purposes it is important that developing neurons fire synchronously while self-organizing into small worlds [40] and neurons prevented from firing synchronously are prone to apoptosis [38].

Traditionally, anatomists have sought to understand cortical order by study of cortical columns [41,42,43,44,45,46]. These are most marked in the primary visual cortex of large primates, and are composed of areas (macrocolumns) made up of cells with short axons [47,48,49] surrounded by localized groups of cells (superficial patch cells) with longer axons forming regular patches of synaptic connections "patch to patch" to their neighbors [50,51,52,53,54,55,56]; the columns and patches together imposing an irregular hexagonal tiling pattern [44,45] or a square pattern where ocular dominance columns occur [56]. In primary visual cortex [57,58, 59] individual neurons show preferential responses for visual stimulation according to the orientation of an elongated, slowly moving visual stimulus. Orientation preference (OP) is organized within the column around a pinwheel singularity, where OP from 0-180 degrees circles the singularity through all 360 degrees [eg 41]. OP also tends to form mirror reversals of the pattern between adjacent columns – most apparent where square ocular dominance columns are present [56]. The longer-axon patch cells, as well as forming patch to patch connections, also tend to link together short-axon cells that have similar OP "like to like" [51,60]. Outside columnar cortex orderliness is much less apparent. Yet, in small animals, where there is little order even in visual cortex, individual cells still show selective responses [61,62], like to like connections [63] and small areas of pinwheel structure [64]. Widely in cortex, whether clearly columnar or not, patch cells make patch to patch connections ubiquitously, forming many overlapping systems [53].

Earlier models for embryogenesis [65,66,67,68,69,70,71,72,73,74,75,76] were unable to provide any complete explanation of why columnar development takes place before visual experience [77] yet requires visual experience to maintain the organized pattern [78,79], nor why OP responses were not simple static responses to lines in the visual field, but varied systematically with the angle of attack, speed, and length of the moving stimulus line [80]. Empirically these effects could be explained by an association of individual neurons' OP to their preferences for spatial and temporal frequencies [81] but the mechanism and functional significance of this dynamic linkage remained unexplained.

1.3 Cortical dynamics

Cortical information exchange has been studied largely via the electroencephalogram (EEG) and its relationship to cell action potential pulses. The spatial EEG is composed of both travelling waves and synchronous activity, and while there is general acceptance of the origin of the EEG from synaptic transmembrane currents [82], there

has been much controversy about the mathematical representation of the large scale wave processes [83,84,85,86,87,88,89,90,91,92,93,94] and their relationship to neuronal group interactions. Singer and colleagues helped to bridge this discontinuity of scale when they discovered that synchronous oscillating pulses around the 40 Hz gamma frequency link cells responding to separate stimulus features [24,25,26,27,28,95]. Synchrony is of importance in cognitive processes [96] and arises from local excitatory/inhibitory interactions [97]. The occurrence of wide fields of synchronous EEG and pulse activity means that, to have large representational capacity, the synchronous states must be somehow spatially partitioned.

Understanding of these phenomena has been improved by their simulation. The power spectrum, frequency/wavenumber characteristics and evoked potentials of the EEG, and pulse synchrony, can all be reproduced using mass action modeling of neural masses [87,88,94,98,99,100,94,101,102,103]. Wave properties in these simulations are near-linear within their realistically low-average firing-rate normal operating range, and consistent properties have been demonstrated directly from electrocortical waves. Autoregression analysis of electrocortical (ECoG) activity exhibits thermal-like near-equilibrium activity, with energy equipartitioned among group resonant modes [86], and coherence analysis of ECoG from closely spaced intradural electrodes shows wave patterns explicable as collisions of travelling waves and the creation of synchronous fields. Spatial damping of the travelling waves is frequency-dependent, in accord with elimination of out of phase components in non-dispersive waves [104,88].

Realistic simulations require bidirectional symmetric connections between neural masses for simulated synchrony to develop, because synchrony is produced by collision of wave-fronts, with dissipation of out-of-phase wave components, and summation of their in-phase components – so signal exchange has to be bidirectionally symmetric to produce a stationary rather than a travelling wave. Yet, although bidirectional couplings occur much more than by chance [33], real neural connections are commonly one-way [34]. This apparent paradox can be resolved, since, in a sparse network with low degrees of separation, polysynaptic pathways of flow between neurons are prolific, allowing transient equilibria of bi-directional polysynaptic flux to create both the wide-spread synchrony seen at the EEG scale and the more restricted synchronies among groups of neurons.

Recent considerations of synaptic dynamics indicate the ways in which transient equilibria may slowly give rise to more established connectivity [105]. Fast (spike-timing dependent plasticity, STDP) modifications, highly sensitive to dynamic adjustment on a short time-scale, pulse spike-to-spike, are continuous on a longer time scale with the Beinenstock-Cooper-Monroe (BCM) rule - itself further subject to slower “floating hook” adaptation. The synapses fast time scale adjustments appear to arise at least in part from competition with each other to establish relative efficacies [36].

It remains necessary to explain how the transient fields of synchrony are related to the mesoscopic anatomical order.

1.4 Scope of theory

We will treat the cerebral cortex as surrounded by a Markov blanket in its interactions with subcortical systems and the external environment – and the cells themselves as each within a Markov blanket, so that cell properties need be considered in minimum necessary detail. Our primary focus will be on intrinsic lateral connections of mesoscopic scale, without concern for the details of organisation in cortical depth, and on the connection profiles in primary visual cortex, but our intention is to formulate a model general enough to apply to all cortical areas.

Our major assumption is that cells that succeed best in competition to survive apoptosis do so by virtue of cell body positions and synaptic couplings that best facilitate synchrony, supporting this assumption from two findings earlier cited - that synchronous firing protects dividing neurons from apoptosis [38] and that dividing neurons self-organize into small-world assemblies [40].

2. Cortical dynamics

2.1 Essential neuronal properties

Mathematical aspects are discussed in Appendix A. The following features are essential:

Summation of pre-synaptic flux at the dendritic membrane leads to zero-lag synchrony [102] - the equilibrium, or "ground state" in which all actively firing excitatory cells fire synchronously and in oscillating interaction with inhibitory cell pulses.

Threshold pulse activation creates a sharp distinction between cells engaged in current network activity versus those currently in a subthreshold state.

Competition among pre-synapses operating on a fast time scale and terminating on the same neuron determines their relative efficacy [36,106]. If the competition is of the "contest" type, rather than the "scramble" type [107] then the fastest firing synapses will shut down activity at other pre-synapses.

2.2 Conditions for synchronous equilibrium

At synchronous equilibrium, pre-synaptic flux is bidirectionally symmetrical, ie:

$$\varphi_{ij}(t) = \varphi_{ji}(t) \tag{1a}$$

where $\varphi_{i,j}$ are pre-synaptic flux rates – the rate of arrival of pulses sent to the pre-synapses terminating on neuron i from neuron j, over all routes, (and vice-versa) weighted by the effective strengths of synaptic connection over all these routes. Expressed in terms of efferent pulses and synaptic gain factors leading to the pre-synaptic flow

$$\rho_{ij}\, g_{ij} \varepsilon_{ij} Q_j\,(t) = \rho_{ji}\, g_{ji} \varepsilon_{ji} Q_i(t) \tag{1b}$$

where $\rho_{ij,ji}$ is number of synaptic connections for monosynaptic relay, and/or the equivalent density of connections over polysynaptic pathways, $g_{ij,ji}$ is the equivalent slowly time-varying synaptic gain, $\varepsilon_{ij,ji}$ that of fast varying synaptic efficacy, and $Q_{j,i}$ are the efferent pulse rates of the two cells.

We will show that symmetry of all factors left and right in Eqn. (1b), maximizing synchrony, determines the patterns of connections emerging during embryogenesis.

2.3 Analogy to equilibrium thermodynamics, and network dynamics

Pre-synaptic flux is physically analogous to electric current, mechanical force, or heat flow. Summing the autocorrelations of all pre-synaptic flows gives a value, A, *the total power of pre-synaptic flux* generated by all cells, while C, the summed cross-correlations of flux between all pairs of cells, is *the total synchronous presynaptic power* (Appendix A). Their difference

$$F = A - C \tag{2}$$

is the power of dissipated pre-synaptic flux and, in steady state conditions, is equal to the power of extrinsic inputs and spontaneous (noisy) pulse generation.

F is analogous to thermodynamic free energy, A to internal energy, and C to energy associated with entropy.

Equation (2) requires that if A is in a steady state, F must be at a minimum if C is at a maximum. This defines a stable equilibrium, or attractor. In anatomical terms this means that stable equilibria are associated with bidirectionally symmetric connectivity and flow, thus maximizing cross-correlation. Conversely, if C is at a minimum, F is at a maximum and an unstable equilibrium exists, associated with asymmetric connectivity and flow. The stable equilibria are synchronous states, the unstable equilibria states with travelling waves; the latter acting as directed vectors between basins of attraction, and thus creating sequences of distinct synchronous states. This identifies the cortical dynamics with a heteroclinic network, exhibiting multi-stability and metastability [108] as distinct from other types of metastability [91].

If bidirectionally symmetric connections increase in number without increase in mean action-potential firing rate, total cross-correlation will increase while autocorrelation remains the same. This implies a progressive reduction in free energy, and should correspond to the emergence of anatomically realistic connectivity, along with subsequent consolidation of learning.

2.4 The curse of dimensionality and distinguishable synchronous steady-states.

If M of N neurons are above threshold then N!/M!(N-M)! steady-states are possible, including stable and unstable equilibria – but how many of these states could be functionally distinct? Representation of the steady-states requires a space of very high dimension, implying a "flat" energy landscape subject to the "curse of dimensionality" [109] – that is, limitation of the states between which distinguishable transitions can take place with sufficient reliability. Thus, learning in the network requires the emergence of distinguishable states of synchrony from a larger set of indistinguishable states, and distinguishability is the inverse of cross-correlated function among separate sets of neurons. Put another way, distinguishable states are more orthogonalized, and thus representable in lower dimension than indistinguishable states.

Both local dynamics, and the anatomical order, bear upon the distinguishability of firing states. Fast changes in synaptic efficacies will transiently partition distinguishable states with very small change in synaptic efficacies,

if the structural and slow synaptic gains are near balance. Since neurons tend to be interconnected with many near neighbors, but also with more widely scattered remote neurons, generally synchrony is high at short range among all cells, and distinguishability correspondingly low, while more distinguishable synchronous states will occur among neurons that are strongly connected but have more remote cell bodies – with implications for the organization of Perlovsky's "crisp" versus "vague" representations.

3. The embryonic process

3.1 Formation of an ultra-small world, in populations of excitatory neurons with disparate axonal lengths.

To aid survival neurons must minimize axonal lengths, forming an ultra-small world [110]. Excitatory cells occur in populations with widely disparate axonal lengths and differing axonal tree densities in different cortical areas [111]. We simplify the cell populations to two types only – a long-axon type we will call alpha cells, and a short-axon type called beta cells. Apoptosis must select short and long axon cells in requisite relative numbers so that the population average axonal density versus distance from cell bodies follows the required ultra-small world inverse power law for degree of separation (see Appendix B). There must then be a distance, X, from their cell bodies, at which alpha and beta cells are of equal axonal density, while at distances less than X beta cells have denser axonal trees and vice versa for alpha cells, influencing their favoured range of synaptic connection accordingly. Symmetry of the factors in equation 1(b) will then emerge as follows:

3.2 Preferential development of bidirectional monosynaptic connections

Monosynaptic connections will always have greater gain than any single polysynaptic pathway, so, if direct reciprocal axodendritic contact between neurons occurs, reciprocal monosynaptic links will tend to form preferentially where LTP timing in the STDP gate, interacting with action potential back-propagation in the dendritic tree [112] provides favourable pre/post-synaptic coincidence.

3.3 Reciprocal selection of fast synaptic gains – $\varepsilon_{ij,ji}$ - in synchronous sets

Reciprocally connected neurons will tend to offer each other reciprocal support in contest competition to establish maximum synaptic efficacies. Transient stable states will occur, in each of which $\varepsilon_{ij} = \varepsilon_{ji}$.

3.4 Reciprocal formation and stabilisation of slow synaptic gains – $g_{ij,ji}$

As symmetric STDP/LTP connections form, and strengthen in accord with the BCM learning rule, the negative feedback "floating hook" BCM property will cause pre-and post-synaptic pulse rates to approach equity, and slow synaptic gain to become equal in each direction of flow.

3.5 Consequent mesoscopic anatomical geometry

The establishment of bidirectionally symmetric synaptic connections maximizing symmetry and synchrony then forces:

- Alpha cells to form reciprocal symmetric synaptic connections, either at very short distances of separation, or at distances of separation of their cell bodies equal to or greater than X, necessitating

aggregation of their cell bodies closely together, and the formation of patch-like connections at distances, $0, X, 2X, \ldots$ Regular tiling in hexagons, squares or triangles can develop, or irregular tiling in combinations and overlaps of these basic forms.

- Beta cells to form synaptic connections at all distances less than X, creating local clusters of cells.
- Synaptic connections between alpha and beta cells to develop at distances of separation equal to X, creating rings of reciprocal connection of radius X around each alpha cluster, amongst the neighboring clusters of beta cells. Alpha/beta connections necessarily resemble 1:1 projections of a Euclidean plane to interlocking and cross-connected Mobius strips (see Appendix B) as the unique way that synchronous resonance can attain maximum.
- And to further maximize resonance the adjacent beta clusters must receive projections from each other that approach mirror images.

Growth simulations confirm the creation of these patterns.

3.6 Growth simulations

Figure 1 shows the outcome of growth simulations [113,114] using a mechanical force-equilibrium algorithm exploiting the physical analogy of mechanical force and pre-synaptic flux, to determine, firstly, cell body positions consistent with ultra-small world configuration, then those subsequently establishing synaptic connectivity so as to maximise symmetric synaptic flux at equilibrium – that is, the cells that would survive apoptosis. A spectrum of outcomes develop from columnar to seemingly random, and although simulation outcomes can be quite different depending on the relative lengths of alpha and beta axons, the random-appearing outcomes are poorly resolved, but structurally equivalent to the columnar outcomes.

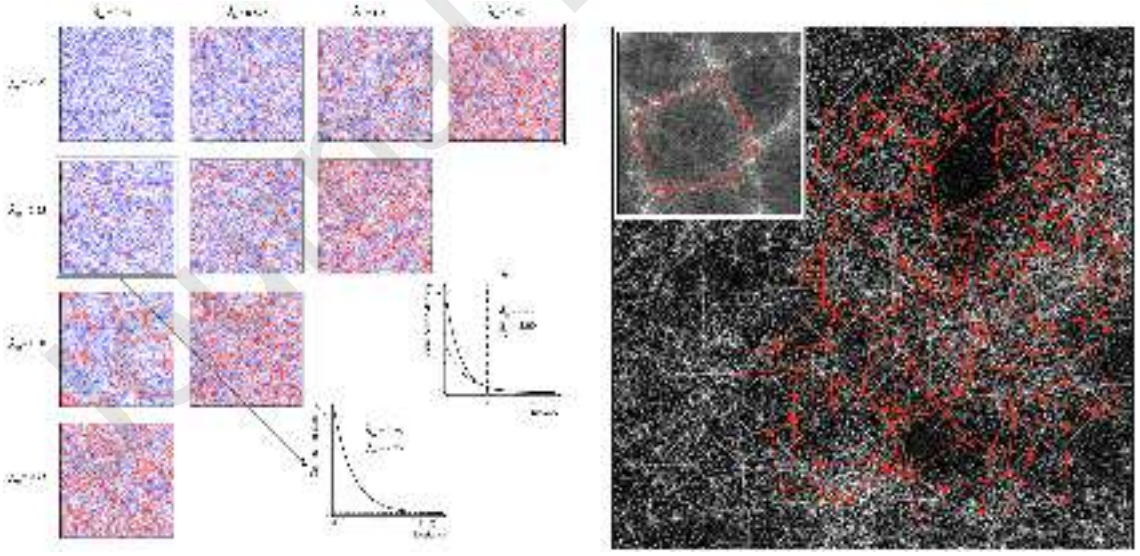

Figure 1.
Left. Growth simulations
Optimum cell positions for survival of alpha (long axon, red) and beta (short axon, blue) pyramidal cells.

Outcomes are shown as functions of the axonal length of the cell types available for selection. Y-axis, beta cell axonal lengths decrease ($1/\lambda_\beta$). X-axis, alpha cell axonal lengths decrease ($1/\lambda_\alpha$).
Inset black and white graphs show representative examples of the population density of alpha and beta cell axonal trees as functions of distance from cell bodies, marked at a distance, X, at which the density of their axonal trees is equal.
Right. Similarity of structure in columnar and non-columnar growth.
A non-columnar growth simulation outcome, with a columnar outcome inset. Beta cells form the black background, and white dots and lines alpha cells and connections. The distance, X, has been is normalised in the two instances and alpha cells separated by distance X highlighted in red.

Figure 2 displays the way outcomes of simulation approximate real anatomy. Alpha cells can now be identified with superficial patch cells, and beta cells with local groups of short axon cells. The ubiquitous organization of patch-to-patch and like-to-like connectivity, the organization of short-axon cells within column centers, the organization of OP for slowly moving lines in monocular cortex and ocular dominance columns with OP pinwheels ranging 0-180 degrees over 360 degrees around singularities, the occurrence of OP linear zones and saddles, and mirror refection of OP particularly in ocular dominance columns – all are accounted for.

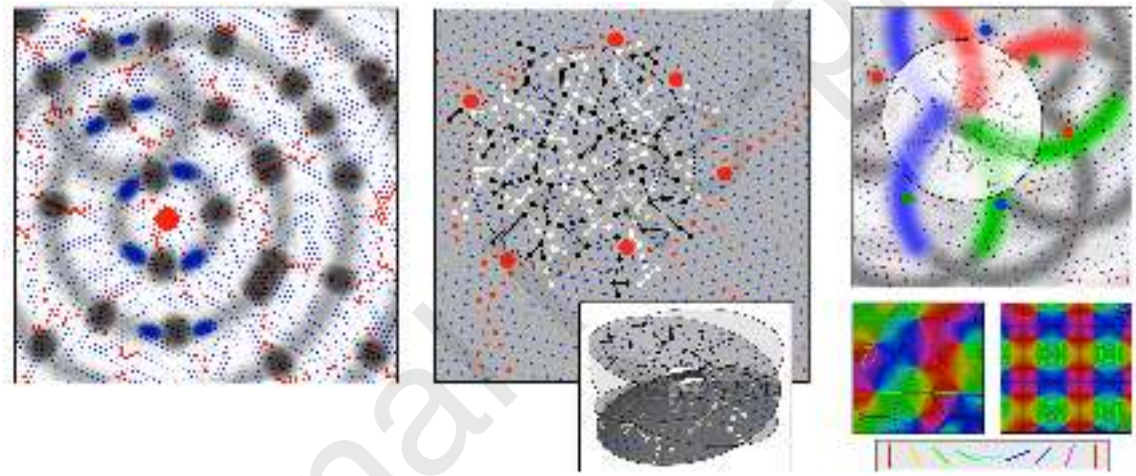

Figure 2.
Left. Superficial patch cells.
A representative alpha cell (large red central spot) and patch connections. Surrounding zones of potential synaptic connection with other alpha cells have been delineated in light grey concentric circles. Dark grey patches occur where other alpha cells are positioned and able to make reciprocal connections, alpha to alpha, creating regularly spaced, typical patch cell connectivity. Alpha/beta synapses maximizing resonance with the central alpha cell with stimulation of a particular angular domain are shown as darkened blue areas of "like to like" connections.
Middle. Local connectivity.
From the same simulation, sparse beta cell connections consistent with the findings of Song et al. [34] have been marked in black or white, showing how interweaving networks occur. Some connections (shown as black and white dashed connections) result in partial closure rather than complete independence of the interpenetrating networks, so that structures analogous to sets of interconnected Mobius strips arise – as shown in the inset.
Right. Reciprocal connections of patch cells to local cells.
Top: fields of synaptic connections from alpha cells to beta cells are coloured red, green, and blue according to their origins from diametrically opposite, similarly coloured, alpha cells. These

opposite cells establish synapses at similar angles from the centre of the network of beta cells, on interpenetrating, but distinct parts of the beta cell network.
Bottom: shows how wide development of alpha/beta connectivity, in accord with the top diagram, results in the creation of an OP map for slowly moving lines of a particular orientation shown in the colour/orientation key. With alpha cells in hexagonal array (left) patterns of neuron orientation preference seen in monocular visual cortex arise with imperfect reflection of OP between macrocolumns. With alphas in square array (right), orientation preference crosses column boundaries orthogonally, in mirror reflections typically seen in ocular dominance columns.

4. Mature cortical function

4.1 Post-natal modification

After birth, the cortex must learn to assimilate sensory inputs and construct motor outputs, for which the ante-natal synaptic framework provides an anatomically organized, rather than a random, scaffold.

Taking the visual system as representative, images of a moving object received over sensory pathways are relayed by lateral patch connections to several macrocolumnar systems (local maps). The inputs to the local maps form a set of spatial and temporal samplings of the moving image over a short epoch, creating synchrony and favoring new synapse formation, so the two dimensions of spatial position and the two dimensions of velocity in the X and Y axes of the input stimulus become sampled into static synaptic connections, within the x and y axes of each of a set of clusters of beta cells (see Appendix C). Symbolically, as sets of samples in space and time

$$X, Y, \{t - \Delta t\} \rightarrow \{x, y\}, t$$

This explains why columnar structure, although it appears antenatally without structured input, requires post-natal structured input to retain its structure. Simulations of the relay of signals in this manner [113] account for the variation of OP with angle of attack, speed, and length of visual stimulus lines described by Basole et al., [80] - findings that contradicted earlier models of response preference emergence. The association of OP with spatial and temporal frequency preferences described by Issa et al. [81], is the Fourier representation of the effect.

Conversely, by reversal of the directions of signal flow, static patterns of synaptic connections may be read out in response to focal activation by other learned inputs, as temporally organized patterns.

$$\{x, y\}, t \rightarrow X, Y, \{t + \Delta t\}$$

Thus, representations must progressively evince a high mutual information with representations in other cortical areas and the environment, the whole becoming a description of a unique experience of an environment's specific spatio-temporal character, and of the individual's sensing, doing and being, within that environment.

The *synaptic patterns* move far from equilibrium in the sense of Prigogine [115,116], so although short-term pulse and wave dynamics remain near equilibrium, free energy is progressively minimized, but entropy bounded (See Appendix C).

Figure 3 illustrates the formation of neural representations in synchronous sets in primary cortex, indicating that multiple neural representations, each of a slightly different stimulus, and each therefore of slightly different orientation and translations, and of either chirality, form in local interareal networks. Then relay to a secondary cortical area by topologically ordered, divergent and reciprocal cortico-cortical fibers results in spread via superficial patch fibers to local maps in a similar way to lateral spread in the primary cortex. Although all resemblance to the original sensory image appears lost in the secondary cortex representations, images have formed that preserve neighborhood relations in each of many diverging representations, spatially mixed with each other. Within the sparse connection system it can be seen that + and x marks, closely situated in the stimulus, become replicated when copied to many locations – but in each replicate, + and x remain closely adjacent, preserving topological identity.

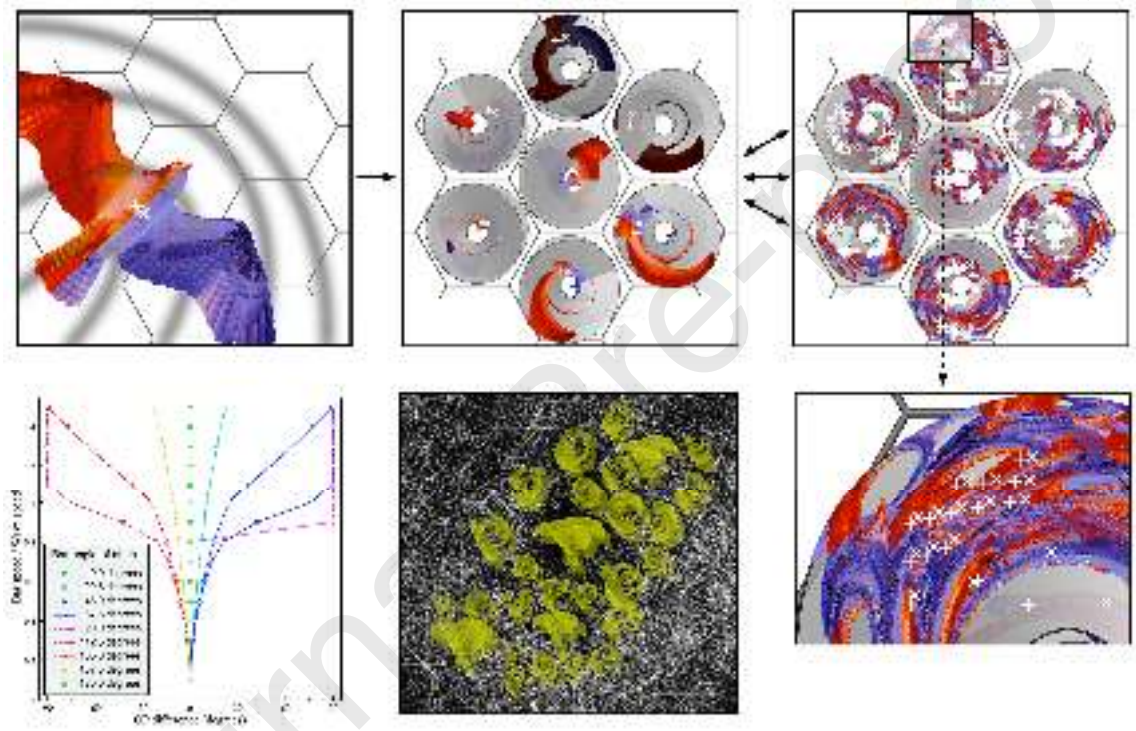

Figure 3. Representations and their relay within and between cortical areas.
(This figure is schematic. No attempt has been made to represent the geometric transformations of an input image between retina and visual cortex.) Closely situated positions on an input stimulus are followed to their multiple representations in primary cortex, and onwards by cortico-cortical fibres to a secondary cortical area, where they undergo a second dispersal to multiple representations at the higher level.
Top left: A stimulus (the image of an eagle moving across the visual field) is projected to primary sensory cortex by classical pathways. Lateral waves (shown as half-tones around the projection of the eagle) are propagated via the superficial patch connections. Two closely situated positions on the initial stimulus are designated by white + and x.
Top middle: Dispersal to multiple synchronous fields in primary cortex creating multiple images as 1:1 projections of the input stimulus to each of the beta clusters, with conduction lags.
Top right. After relay via divergent cortico-cortical fibres, further fields of synchrony are created in a secondary cortical area.

Bottom left: Results from simulations showing that apparent orientation preference of neurons varies systematically from the classical slowly-moving visual line result, with both the angle of attack of the moving bar and the speed with which the bar is moving.
Bottom middle: Superimposed on a growth simulation background as yellow patterns, are pools of cells with synaptic linkages learned in response to their synchronous activation. Overlapping with each other within the sparse system of cellular connections, each represents a slightly different learned sample of a stimulus.
Bottom right: Enlargement of a small segment of the activity at secondary cortical level, showing that topological identity, despite transformations and superpositions, is retained in the projections of the image initially delivered to the retina.

4.2 Cortical computation and adaptive learning

The almost coincident synaptic representations and the arrangement of interweaving connections demonstrated in Figure 3 are in line with Perlovsky's dynamic logic. Throughout cortex, small locales store closely similar, continuously varying, bi-chiral, synaptic images. These locales are connected by longer-range cortico-cortical connections in a network of networks. Section 2.4 indicated that closely situated, and closely similar patterns of activation would be essentially indistinguishable consequent to the curse of dimensionality - or equivalently, each of the indistinguishable patterns might be regarded as concurrently active. Conversely, connections between distant locales may form synchronous systems that are more clearly distinguishable. This would permit parallel search toward a well distinguished synchrony maximum - a substrate for Perlovsky's concept of the fusion of "vague" images higher and lower in the cortical information stream, into "crisp" images. In formation of the "crisp" image, the higher dimensional "vague" images fuse to a single, lower dimensional representation – a process well suited to optimization problems and similar to computation by entanglement among quantum states.

Given this powerful means of associative learning, the free energy principle is itself sufficient to establish minimized surprise - but animals must also operate to maximize reward and enhance their survival. Innate subcortical mechanisms selectively consolidating species-appropriate learning and exerting cortex-wide control may perform this function [117,118,119,120,121,122]. Acting via transhypothalamic neurons, these systems reinforce synaptic consolidation on the basis of temporal contiguity, and survival relevance, rather than cortical locality. Thus the imperfect partitioning of "vague" images would enable multiple trials of learning to establish learning optima for organism survival, fusing the individual's innate preferences with individual experience of causal relations in the environment, and of the individual's actions.

5. Conclusion

5.1 Unity of fundamental principles and the mesoanatomy of the cortex.

We have shown, starting from simple and well-established neuron properties, along with an assumed role of synchrony in shaping the outcomes of apoptosis, that much of the millimetric anatomy of the cortex can be explained. To the best of our knowledge the range of findings regarding mesoscopic anatomy and single unit selective responses, unified with simulations and experimental observations of synchrony and the EEG, is not achieved by any other theoretical account, nor do any specifically contradictory experimental data exist. Millimetric anatomical structures appear to be generated by, and are just those necessary, to permit near-equilibrium, multi-stable, electrocortical dynamics. As the developing brain steadily increases the number of

bidirectional monosynaptic connections, a system of synchronous attractors forms. Free energy is minimised, and the system degrees of freedom diminish, as anticipated in the free energy principle. In post-natal life, this process continues, but is directed into specific learning, based upon sensory experience and selection by internal mechanisms.

Response properties become organised in a systematic way that preserves adjacency of closely related synaptic representations, offering a basis for cortical computation via the rapid gradient descent on synchrony with further dimensional reduction, minimizing computational complexity consistent with dynamic logic, while the strengthening of selected synapses sets an upper bound on the entropy of the sensory states that are represented.

The complementarity of both Friston's and Perlovsky's theoretical work with the present work mutually supports all three, and together they constitute an elementary account of basic cortical organization.

5.2 Some comparisons with existing AI

Hopefully this account further assists comparisons between computational neuroscience and systems biology [123]. The filtering properties of individual neurons resemble those applied in convolution neural networks (CNNs) that utilize properties of feature filtering in primary visual cortex neurons discovered over fifty years ago [58], but the filtering properties have additional capacity for generalized representation and association of spatio-temporal stimulus patterns, and abstracted combinations of these at higher levels, while maintaining topological order. It is this orderliness that permits the matching of "vague" images into "crisp" form – a property not generally characteristic of conventional architectures, and perhaps more suitable for embodied operation. Fixed points of the oscillating synchronous field are analogous to the point-attractors with constant neuron firing rate states of CNNs and attractor neural networks (ANNs) [124]. Cortico-cortical relays play the same role as ascribed to feed-forward projection in perceptrons [125] with the added property of feedback to the input layer as introduced to CNNs by Sabour et al [126]. No direct equivalent of the back-propagation algorithm [127] is apparent, but the establishment of selected reciprocally resonant sets between cortical areas may have much the same effect.

5.3 Further testing

The relative lengths of axonal connections at millimetric scale in different cortical areas have not yet been estimated with sufficient precision to show that the degree of column formation shown in our growth simulations actually matches the variations in real cortex. Axonal lengths are distributed, rather than conforming closely to our assumption of distinct long and short-axon populations, but this does not pose any fundamental objection to the model. A relatively easily tested prediction, in primary visual cortex, is that long- axon patch connections should terminate on short-axon cells in the predicted 1:1 mapping topology. That is, patch connections reaching "like to like" from patch cell bodies on opposite sides of a column should terminate on different cells, yet all upon cells with common orientation preference. A more elaborate opportunistic experiment on the conformation of receptive fields in closely situated cells in primary sensory cortex has yielded supportive results [128].

The generation of co-synchronous fields in cortex also appears likely to produce effects observed by fMRI/MEG in support of Perlovsky's computer modelling. Repeating the experimental protocol of Bar et al, [16,17], instead using coherence and phase estimates of EEG as the outcome measure, could establish the essential analogy of the artificial and proposed real networks.

Appendices

Appendix A. Dynamics

State equations for polysynaptic signal flow in cortical neurons.

Generation of pre-synaptic flux

$$\varphi_{ij}(t) = \pm g_{ij}\varepsilon_{ij}\rho_{ij}A_{ij}\left(t - \frac{|i-j|}{v} - \tau\right) * Q_j\left(t - \frac{|i-j|}{v}\right) \quad \text{(A1)}$$

φ_{ij} is pre-synaptic flux conveyed from the j-th to the i-th neuron by polysynaptic relay, including monosynaptic relay as a special case.

Q_j is the efferent pulse rate of the j-th neuron.

v is the speed of conduction between j and i over monosynaptic connections (if any).

The convolution $A_{ij}\left(t - \frac{|i-j|}{v} - \tau\right) * Q_j\left(t - \frac{|i-j|}{v}\right)$ expresses effects of delayed arrival of pulse transmission through the polysynaptic pathways joining j to i, and may itself be time-varying.

± indicates whether the net effect of the pre-synapse(s) is inhibitory or excitatory.

ρ_{ij} is number of synaptic connections from j to i, for monosynaptic relay, or the equivalent gain over polysynaptic pathways, or the summed gain over both types..

g_{ij} is slow time-variation value of synaptic gain [105,129,130].

ε_{ij} is fast-variation synaptic efficacy, subject to pre-synaptic "contest" competition, with outcomes determined by minima of

$$E_i(t) = \sum_{ij,ik} B_{jk}\varphi_{ij}\varphi_{ik} + \sum_j \varepsilon_{ij}\varphi_{ij} \quad \text{(A2)}$$

B_{jk} describe the competitive and cooperative interactions of synapses carrying pulses from neurons j and k on the afferent dendritic membrane, and steady-state efficacies, ε_{ij}, of the afferent synapses are given as

$$\varepsilon_{ij} \in \{\varepsilon_{ij}\} = \arg\min E$$

Post-synaptic depolarisation.

$$V_i(t) = D(t-\tau) * (\varphi_{i0} + \sum_j \varphi_{ij})(t) \quad \text{(A3)}$$

V_i is the post-synaptic potential generated by afferent synaptic flux in the i-th neuron.

The convolution $D(t-\tau) * (\varphi_{i0} + \sum_j \varphi_{ij})(t)$ expresses the effects of delays due to dendritic conduction in the relay of synaptic potentials to pulse generation.

φ_{i0} is afferent flux to the i-th neuron from external sources.

Generation of action potentials

$$Q_i(t) = f_\theta\big(V_i(t)\big) \tag{A4}$$

Q_i is the efferent pulse rate of the i-th neuron.

f_θ is a sigmoid-like function including effects of reversal potentials, receptor adaptations, and threshold for pulse generation.

Generation of synchrony and minimization of free energy.

Where $\Phi_{ij,ji}$ are the sums of synaptic flux in opposite directions of flow between all pairs of neurons, their difference can be expressed as a Lagrangian

$$L = \Phi_{ij} - \Phi_{ji} = \left(\left(+\Phi_{ij}^{ee}\right) - \left(+\Phi_{ji}^{ee}\right)\right) + \left(\left(-\Phi_{ij}^{ii}\right) - \left(-\Phi_{ji}^{ii}\right)\right) + \left(\left(-\Phi_{ij}^{ei}\right) - \left(+\Phi_{ji}^{ie}\right)\right) \tag{A5}$$

Superscripts ee, ii, ie, ei indicate flux between excitatory and inhibitory cells respectively.

According to the principle of least action the system is in equilibrium when $L \to 0$, requiring

$$\begin{aligned} +\Phi_{ij}^{ee}(q,\dot{q})(t) &= +\Phi_{ji}^{ee}(q,\dot{q})(t) \\ -\Phi_{ij}^{ii}(q,\dot{q})(t) &= -\Phi_{ji}^{ii}(q,\dot{q})(t) \\ -\Phi_{ij}^{ei}(q,\dot{q})(t) &= +\Phi_{ji}^{ie}(-q,-\dot{q})(t) \end{aligned} \tag{A6}$$

where $q, \dot{q}$ represent displacements from mean levels of pre-synaptic flux, and their velocities of displacement. These conditions are met when all cells fire with constant pulse rates, or excitatory cells fire synchronously, inhibitory cells fire synchronously, and excitatory and inhibitory cells fire with a 180 degree phase difference.

For n directed synaptic flows between pairs of neurons,

$$A = \frac{1}{2}\sum_{ij}^{n}\frac{1}{T}\int_0^T \varphi_{ij}^2(t)dt \tag{A7}$$

is the half-power of pre-synaptic flux generated by all cells. The cross-correlation function for all pairs of cells

$$C = \sum_{ij,ji}^{\frac{n}{2}}\frac{1}{T}\int_0^T \varphi_{ij}(t)\varphi_{ji}(t)dt \tag{A8}$$

is the total synchronous pre-synaptic power. The difference

$$F = A - C \tag{A9}$$

is analogous to thermodynamic free energy, A to internal energy, and C to energy associated with entropy.

Appendix B. The developmental process

Formation of an ultra-small world, in populations of excitatory neurons with disparate axonal lengths

Where there are two discrete short-axon and long-axon populations, the cells surviving initial apoptosis must do so in proportions satisfying an inverse power law for the average density versus range from their cell bodies (as proxy for degrees of separation) of their axonal trees, and do so with individual axonal trees that decline in density exponentially with distance – ie

$$\rho_{ij,ji} \propto |i-j|^{-2} \approx N_\alpha \lambda_\alpha e^{-\lambda_\alpha |i-j|} + N_\beta \lambda_\beta e^{-\lambda_\beta |i-j|} \tag{B1}$$

where

N_α is the fraction of excitatory neurons with longer axons (alpha cells)

N_β is the fraction of excitatory neurons with shorter axons (beta cells)

λ_α is the inverse length of the longer axons

λ_β is the inverse length of the shorter axons

Development of local maps

At an axonal range

$$X = \frac{ln\left(\frac{N_\alpha \lambda_\alpha}{N_\beta \lambda_\beta}\right)}{\lambda_\alpha - \lambda_\beta} \tag{B2}$$

the population density of alpha and beta cell axonal trees is equal. Projection of alpha cells to each of the beta networks as resonant 1:1 maps can be represented as projection of a Euclidean plane to Reimann surfaces:

$$P \rightarrow \left\{p = \pm p' \left(\frac{(P-p_0)^n}{|P-p_0|^{n-1}}\right) + p_0\right\} \tag{B3}$$

where P are complex-number network positions of alpha cell bodies, p are network positions of beta cell bodies within a cluster centered at p_0, and $\pm \mathrm{p}'$ determines the chirality, scale and orientation of each *local map.* with magnitude of p'proportional to X, and the diameter of each beta cluster approximately $2X$.

The order, n, is the multiplication of angle in the P plane to angle of projection onto the Riemann surface – and, equivalently, the number of times the beta cell network is folded within itself before the network closes, and thus also a measure of the number of synaptic contacts that can be made in a continuous network. Realistically, such networks would not be ideal, but partially closed, and cross-linked with other partially formed networks.

Since alpha-beta connections are made in arcs of radius X, the connections from alpha cells diagonally opposite from each other across a beta cell cluster must project connections to beta cells close to a perpendicular diagonal - that is, $p' \propto \sqrt{-1}\,X$ - a condition met only for positive integer values in n. For n = 1, $+P \rightarrow +p$ and $-P \rightarrow -p$, and the input maps take simple Euclidean form. For n = 2, $+P \rightarrow +p$ and also $-P \rightarrow +p$, and the maps are projections of a Euclidean plane onto a Mobius strip For n = 3, 5, 7…, and for n = 4, 6, 8…, respectively, redundant, overlapping, and cross-linked, Euclidean-like, or Mobius-like solutions can exist. Because of their collectively greater continuous extent of beta cell connections, maximum resonance requires an ensemble of cross-linked Mobius, and Mobius-like, mappings to form.

Adjacent maps must have opposite chirality, and receive projections from each other that approach mirror images, so

$$p_1' \approx -p_2' \tag{B4}$$

in adjacent local maps, 1 and 2.

Appendix C. Post-natal cortical function

Intra-areal interactions – storage and readout.

Images of a moving object, O, projected to primary cortex over sensory pathways and relayed by lateral patch connections to each of the local maps, can be represented by

$$O\left(P, t - \frac{|P-p|}{\upsilon}\right) \rightarrow \{o(p)\}, (t) \tag{C1}$$

Where υ is the electrocortical wave velocity.

The two dimensions of spatial extension and the two dimensions of velocity in the X and Y axes of the input stimulus become compressed to two dimensions of static synaptic connections

– viz:

$$O\left(K_x, K_y, V_x, V_y\right) \rightarrow \left\{o\left(k_x, k_y\right)\right\} \tag{C2}$$

where K_x, K_y, V_x, V_y are the extensions and velocities of stimulus movement in the X and Y axes of receptor cortex at the large scale, and k_x, k_y are extensions of the image formed in a given local map by the resulting synchronous field.

Doppler shift in the relay of waves via the superficial patch system alters the metric of the local representations:

$$k_x \propto \frac{\upsilon}{\upsilon \pm V_x} K_x$$

and

$$k_y \propto \frac{\upsilon}{\upsilon \pm V_y} K_y$$

This process is capable of operating in reverse,

$$\{o(p)\},(t) \rightarrow O\left(P, t + \frac{|P - p|}{v}\right) \quad \text{(C3)}$$

permitting reading a stored synaptic pattern into a timed sequence of output.

Learning and bounded entropy

The effect of learning is to strengthen specific bidirectional connections, contributing to the magnitude of cross-correlations (eqn A8) relative to the autocorrelations (eqn A7). So, as learning progresses, entropic energy increases, and free energy decreases. Concurrently, learned behaviors become more probable than equiprobable random behaviors, and some behaviors very improbable - so that entropy decreases, moving from Boltzmann-like,

$$S = k_B ln\Omega$$

where Ω is the number of equiprobable synchronous states, to Gibbs-like,

$$S = k_b \sum p_i \, lnp_i$$

where p_i are the (unequal) probabilities of the learned states.

Acknowledgements

This work received long-term support including that of the New Zealand, Australian and United Kingdom Medical Research Councils, the Frank Hixon Fund of the California Institute of Technology, the MHRF and Wellcome Trust in the UK, and the Oakley, Ross and Pratt Foundations of Australasia. It is dedicated to the memory of Adrienne Edith Wright.

References

1 Sherrington CS. The Integrative Action of the Nervous System. Yale University Press; 1906.

2 Young JZ. A Model of the Brain. Oxford, the Clarendon Press; 1964.

3 Hebb DO. The Organization of Behavior. John Wiley; 1949.

4 Edelman G. Neural Darwinism. The Theory of Neuronal Group Selection. Basic Books; 1987.

5 Domingos P. The Master Algorithm. Basic Books; 2015.

6 Friston K. A theory of cortical responses. Philosophical Transactions of the Royal Society B. 2005; 360: 815-836.

7 Friston K. The free energy principle: a unified brain theory? Nature Reviews Neuroscience.2010;11: 127 – 138. doi:10.1038/nrn2787.

8 Friston K, Thornton C, Clark A. Free energy minimization and the dark room problem. Frontiers in Psychology 2012; doi:10.3389/fpsyg.2012.00130.

9 Clark A. Whatever next? Predictive brains, situated agents, and the future of cognitive science. Behavioral and Brain Sciences 2013; 36: 181-253. doi:10.1017/S0140525X12000477.

10 Ramstead MJD, Badcock PB, Friston K. Answering Schroedinger's question: a free energy formulation. Physics of Life Reviews 2018; 24: 1-16. http://dx.doi.org/10.1016/j.plrev.2017.09.001.

11 Sengupta B, Tozzi A, Cooray GK, Douglas PK, Friston K. Towards a neuronal gauge theory. PLOS Biology 2016; doi: 10.1371/journal.pbio.1002400.

12 Jaynes ET On the rationale of maximum entropy methods. Proceedings of the IEEE 1982; 70: 939-952.

13 Akaike H.A new look at the statistical model identification. IEEE Transaction in Automatic Control 1974;19: 716-723.

14 Friston K. A free energy principle for a particular physics. eprint 2019; arXiv:1906.10184.

15 Perlovsky LI., McManus MM. Maximum likelihood neural networks for sensor fusion and adaptive classification. Neural Networks 1991; 4: 89–102. doi: 10.1016/0893-6080(91)90035-4.

16 Perlovsky LI, Deming RW, Ilin R. Emotional Cognitive Neural Algorithms with Engineering Applications; Dynamic Logic: From Vague to Crisp. Heidelberg: Springer; 2011.

17 Perlovsky LI. Physics of the Mind. Front. Syst. Neurosci. 2016; 10:84. doi: 10.3389/fnsys.2016.00084

18 Perlovsky LI. Neural Networks and Intellect: Using Model-Based Concepts. New York, NY: Oxford University Press;2001.

19 Russell S, Norvig P. Artificial Intelligence: A Modern Approach, 3rd Edn. Pearson; 2010.

20 Bar M, Kassam KS, Ghuman AS, Boshyan J, Schmid AM, Dale AM, et al.. Top-down facilitation of visual recognition. Proc. Natl. Acad. Sci. U.S.A. 2006; 103: 449–454. doi: 10.1073/pnas.0507062103.

21 Kveraga K, Ghuman AS, Bar M. Top-down predictions in the cognitive brain. Brain Cogn.2007; 65: 145–168. doi: 10.1016/j.bandc.2007. 06.007.

22 Yamins DLK., DiCarlo JJ. (2016) Using goal-driven deep learning models to understand sensory cortex. Nature Neuroscience 2016; 19: 356 – 365 doi:10.1038/nn.4244.

23 Friston K, Adams RA, Perrinet L, Breakspear B. Perceptions as hypotheses: saccades as experiments. Front. Psychol. 2012; doi.org/10.3389/fpsyg.2012.00151.

24 Eckhorn R, Bauer R, Jordon W, Brosch M, Kruse W, Monk M, Reitboeck HJ. Coherent oscillations: a mechanism of feature linking in the in the visual cortex? Biological Cybernetics 1988; 60: 121–130.

25 Eckhorn R, Reitboeck HJ, Arndt M, Dicke P. Feature linking via synchronization among distributed assemblies: simulations of results from cat visual cortex. Neural Computation 1990; 2: 293-307.

26 Gray CM, Singer W. Stimulus-specific neuronal oscillations in orientation columns of cat visual cortex. Proceedings of the National Academy of Science, USA 1989; 86: 1698-1702.

27 Singer W. Putative functions of temporal correlations in neocortical processing. In Large-scale Neuronal Theories of the Brain, (p.201-237). MIT Press; 1994.

28 Singer W. Neuronal synchrony: a versatile code for the definition of relations? Neuron 1999; 24: 49-65.

29 Bagnard D, Lohrum M, Uziel D, Puschel AW, Bolz, J. Semaphorins act as attractive and repulsive guidance signals during the development of cortical projections. Development 1998; 125: 5043-5053.

30 Goldberg JL. How does an axon grow? Genes and Development 2003; 17:941-958. doi:10.1101/gad.1062303.

31 Meyer G. Genetic Control of Neuronal Migrations in Human Cortical Development. Springer; 2007.

32 Blackmore MG, Moore DL, Smith RP, Goldberg JL, Bixby JL, Lemmon VP. High content screening of cortical neurons identifies novel regulators of axon growth. Mol Cell Neurosci. 2010; 44:43-54. doi:10.1016/j.mcn.2010.02.002.

33 Perin R, Berger TK, Markram H. (2011) A synaptic organizing principle for cortical neuronal groups. PNAS USA 2011; 108: 5419-5424. doi.org/10.1073/pnas.1016051108.

34 Song S, Sjostrom PJ, Reigl M, Nelson S, Chklovskii DB. Highly non-random features of synaptic connectivity in local cortical circuits. PLOS Biology 2005; 3(10) e350 doi.org/10.1371/journal.pbio.0030350.

35 Feldman DE. The spike timing dependence of plasticity. Neuron 2012; 75: 556-571. doi: 10.1016/j.neuron.2012.08.001.

36 Markram H, Tsodyks M. Redistribution of synaptic efficacy between neocortical pyramidal neurons. Nature 1996; 382: 807-810.

37 Elmore S. Apoptosis: a review of programmed cell death. Toxicol Pathol. 2007; 35:495-516. doi:10.1080/01926230701320337.

38 Heck N, Golbs A, Riedemann T, Sun J-J, Lessmann V, Luhmann HJ. Activity dependent regulation of neuronal apoptosis in neonatal mouse cerebral cortex. Cerebral Cortex 2008; 18: 1335–1349.

39 Yamaguchi Y, Miura M. Programmed cell death in neurodevelopment. Developmental Cell Review 2015; doi.org/10.1016/jdevcel.2015.01.019.

40 Downes JH, Hammond MW, Xydas D, Spencer M, Becerra VM, Warwick K, Whalley BJ, Natsuto SJ. Emergence of a small-world functional network in cultured neurons. PLOS Computational Biology 2012; 8:e1002522. doi: 10.1371/journal.pcbi.1002522.

41 Bosking WH, Zhang Y, Schofield B, Fitzpatrick D. (1997). Orientation selectivity and the arrangement of horizontal connections in tree shrew striate cortex. Journal of Neuroscience 1997; 17: 2112–2127.

42 Kaschube M, Schnabel M, Löwel S, Coppola DM, White LE, Wolf F. Universality in the evolution of orientation columns in the visual cortex. Science 2010; 330: 1113.

43 Horton CH, Adams DL. The cortical column: a structure without a function. Philosophical Transactions of the Royal Society, London 2005; 360: 837–862.

44 Muir DR, Da Costa NMA, Girardin CC, Naaman S, Omer DB, Ruesch E, Grinvald A, Douglas RJ. Embedding of cortical representations by the superficial patch system. Cerebral Cortex 2011; 21: 2244–2260.

45 Paik S.-B., Ringach DL. Retinal origin of orientation maps in visual cortex. Nature Neuroscience 2011; 14: 919–925.

46 Keil W, Kaschube M, Schnabel M, Kisvarday ZF, Lowel S, Coppola DM, White LE, Wolf, F. Response to comment on “Universality in the evolution of orientation columns in the visual cortex”. Science 2012; 336: 413 doi:10.1126/science.1206416.

47 Sharma J, Angelucci A, Rao S, Sur M. Relationship of intrinsic connections of orientation maps in ferret primary visual cortex: iso-orientation domains and singularities. Presented at Society for Neuroscience, San Diego, California; 1995.

48 Yousef T, Toth E, Rausch M, Eysel UT, Kisvarday ZF. (2001). Topography of orientation centre connections in the primary visual cortex of the cat. Neuroreport 2001; 12: 1693-1699.

49 Buzás P, Kovács K, Ferecskó AS, Budd JML, Eysel UT, Kisvárday ZF. Model-based analysis of excitatory lateral connections in the visual cortex. Journal of Comparative Neurology 2006; 499: 861-881.

50 Gilbert CD, Wiesel TN. Morphology and intracortical projections of functionally characteristic neurons in cat visual cortex. Nature 1979; 280: 120–125.

51 Rockland KS, Lund JS. Intrinsic laminar lattice connections in primate visual cortex. Journal of Comparative Neurology 1983; 216: 303–318.

52 Hirsch JA, Gilbert CD. Synaptic physiology of horizontal connections in the cat's visual cortex. Journal of Neuroscience 1991; 11: 1800–1809.

53 McGuire BA, Gilbert CD, Rivlin PK, Wiesel TN. Targets of horizontal connections in macaque primary visual cortex. Journal of Comparative Neurology 1991; 305: 370–392.

54 Muir DR, Douglas RJ. From neural arbours to daisies. Cerebral Cortex 2011; 21: 1118–1133.

55 Binzegger T, Douglas RJ, Martin KAC. Stereotypical bouton clustering of individual neurons in cat primary visual cortex. Journal of Neuroscience 2007; 27: 12242-12254. doi: 10.1523/jneurosci.3753-07.2007.

56 Obermayer K, Blasdel GG. Geometry of orientation and ocular dominance columns in monkey striate cortex. Journal of Neuroscience 1993; 13: 4114–4129.

57 Hubel DH, Wiesel TN. Receptive fields of single neurones in the cat's striate cortex. Journal of Physiology 1959; 148: 574–591.

58 Hubel DH. Evolution of ideas on the primary visual cortex, 1955-1978: A biased historical account. Nobel lecture, 8 December 1981. Nobel Institute; 1981.

59 von der Malsburg Ch. How are nervous structures organized? In Synergetics of the Brain (p. 238-249). Springer Nature; 1983.

60 Angelucci A, Levitt JB, Lund JS. Anatomical origins of the classic receptive field and modulatory surround field of single neurons in macaque visual cortical area V1. Progress in Brain Research 2002; 136: 373–388.

61 Girman SV, Sauve Y, Lund RD. Receptive field properties of single neurons in rat primary visual cortex. Journal of Neurophysiology 1999; 82: 301–311.

62 Garrett ME, Nauhaus I, Marshel JH, Callaway EM. Topography and areal organization of mouse visual cortex. Journal of Neuroscience 2014; 34: 12587-12600. doi: 10.1523/jneurosci.1124-14.2014.

63 Ko H, Hofer SB, Pichler B, Buchanan KA, Sjostrom PJ, Mrsic-Flogel TD. Functional specificity of local synaptic connections in neocortical networks. Nature 2011; 473: 97-91. doi: 10.1038/nature09880.

64 Van Hooser SD, Heimel JA, Chung S, Nelson SB. Lack of patchy horizontal connectivity in primary visual cortex of a mammal without orientation maps. Journal of Neuroscience 2006; 26: 7680-7692. doi: 10.1523/jneurosci.0108-06.2006.

65 von der Malsburg C. Self-organization of orientation sensitive cells in the striate cortex. Kybernetic 1973; 14: 85–100.

66 Swindale NV. A model for the formation of orientation columns. Proceedings of the Royal Society, London 1982; 215: 211–230.

67 Swindale NV. A model for the coordinated development of columnar systems in primate striate cortex. Biological Cybernetics 1992; 66: 217–230.

68 Swindale NV. The development of topography in the visual cortex: a review of models. Network 1996; 7: 161–247.

69 Tanaka S. Theory of self- organization of cortical maps: mathematical framework. Neural Networks 1990; 3: 625–640.

70 Durbin R, Mitchison G. A dimension reduction framework for understanding cortical maps. Nature 1990; 343: 644–647.

71 Obermayer K, Ritter H, Schulten K. A principle for the formation of the spatial structure of cortical feature maps. Proceedings of the National Academy of Science, USA 1990; 87: 8345–8349.

72 Miyashita M, Tanaka, S. A mathematical model for the self- organization of orientation columns in visual cortex. Neuroreport 1992; 3: 69–72.

73 Grossberg S, Olson SJ. Rules for the cortical map of ocular dominance and orientation columns. Neural Networks 1994; 7: 883–894.

74 Grabska-Barwinska A, von der Malsberg, C. Establishment of a scaffold for orientation maps in primary visual cortex of higher mammals. Journal of Neuroscience 2008; 28: 249 – 257. doi: 10.1523/jneurosci.5514-06.2008.

75 Bauer R, Zubler F, Pfister S, Hauri A, Pfeiffer M, Muir DR, Douglas RJ. Developmental self-construction and configuration of functional neocortical networks.. PLOS Computational Biology 2014; 10: (12) e1003994 doi: 10.1371/journal.pcbi.1003994.

76 Bednar JA. Hebbian learning of the statistical and geometrical structure of visual input. In Neuromathematics of Vision (p.335-366). Springer-Verlag; 2014. doi: 10.1007/978-3-642-34444-28.

77 Wiesel TN, Hubel DH. Ordered arrangement of orientation columns in monkeys lacking visual experience. Journal of Comparative Neurology 1974; 158: 307–318.

78 Blakemore C, Van Sluyters RC. Innate and environmental factors in the development of the kitten's visual cortex. Journal of Physiology 1975; 248: 663–716.

79 Sherk H, Stryker MP. Quantitative study of orientation selectivity in visually inexperienced kittens. Journal of Neurophysiology 1976; 39: 63–70.

80 Basole A, White LE, Fitzpatrick D. Mapping of multiple features in the population response of visual cortex. Nature 2003; 423: 986–990.

81 Issa P, Rosenberg A, Husson TR. Models and measurements of functional maps in V1. Journal of Neurophysiology 2008; 99: 2745–2754.

82 Buzsaki G, Anastassiou CA, Koch C. The origin of extracellular fields and currents – EEG, ECoG, LFP and spikes. Nature Reviews of Neuroscience 2012; 13: 407-420. doi:10.1038/nrn3241.

83 Nunez PL. Neocortical dynamics and Human EEG Rhythms. Oxford University Press; 1995.

84 Robinson PA, Rennie CJ, Wright JJ. Propagation and stability of waves of electrical activity in the cerebral cortex. Physical Review E 1997; 56: 826-841.

85 Wright JJ. Reticular activation and the dynamics of neuronal networks. Biological Cybernetics 1990; 62: 289-298.

86 Wright JJ, Kydd RR, Sergejew AA. Autoregressive models of EEG. Results compared with expectation for a high-order multilinear near-equilibrium biophysical process. Biological Cybernetics 1990; 62: 201-210.

87 Wright JJ, Liley DTJ. Simulation of electrocortical waves. Biological Cybernetics 1995; 72: 347-356.

88 Breakspear M. Dynamic models of large-scale brain activity. Nature Neuroscience 2017; 20: 340 – 352. doi:10.1038/nn.4497.

89 Wilson H R, Cowan JD. Excitatory and inhibitory interactions in localised populations of model neurons. Biophysical Journal 1972; 12: 1 – 24.

90 Freeman W. J. Mass Action in the Nervous System, Academic Press; 1975.

91 Kaneko K, Tsuda I. Chaotic itineracy. Chaos 2003; 13: 926 – 936. http://hdl.handle.net/2215/8486.

92 Moran R, Kiebel S, Stephan KE, Reilly RB, Daunizeau J, Friston KJ. A neural mass model of spectral responses in electrophysiology. Neuroimage 2007; 37: 706 – 720. doi:10.1016/jneuroimage.2007.05.032.

93 Buzsaki G, Freeman WF. (2015) Brain rhythms and dynamic co-ordination. Current Opinion in Neurobiology 2015; 31: v-ix. doi 10.1016/jconb.2015.01.016.

94 Wright JJ, Liley DTJ. Dynamics of the brain at global and microscopic scales: neural networks and the EEG. Behavioral and Brain Sciences 1996; 19: 285-295.

95 Singer W. Cortical dynamics revisited. Trends in Cognitive Neuroscience 2013; 17: 616-626. doi:10.10.1016/j.tics.2013.09.006.

96 Varela F, Lachaux J-P, Rodriguez E, Martinerie J. The brainweb: phase synchronization and large-scale integration. Nature Reviews of Neuroscience 2001; 2: 229-239. www.nature.com/reviews/neuro

97 Buzsaki G, Wang X-J. Mechanisms of gamma oscillations. Annual Review of Neuroscience 2012; 35: 203-225. doi:10.1146/annurev-neuro-062111-150444.

98 Robinson PA, Rennie CJ, Wright JJ. Synchronous oscillations in the cerebral cortex. Physical Review E 1998; 57 :4578-4588.

99 Robinson PA, Rennie CJ, Wright JJ, Bahramali E, Gordon E, Rowe DL. Prediction of electroence-phalographic spectra from neurophysiology. Physical Review E 2001; 63: 021903.

100 Rennie CJ, Robinson PA, Wright JJ. Unified neurophysical model of EEG spectra and evoked potentials. Biological Cybernetics 2002; 86: 457-471.

101 Wright JJ, Bourke PD, Chapman CL. Synchronous oscillation in the cerebral cortex and object coherence: simulation of basic electrophysiological findings. Biological Cybernetics 2000; 83: 341–353.

102 Chapman CL, Bourke PD, Wright JJ. (2002). Spatial eigenmodes and synchronous oscillation: coincidence detection in simulated cerebral cortex. Journal of Mathematical Biology 2002; 45: 57–78.

103 Wright JJ. Work Toward a Theory of Brain Function, (Thesis, Doctor of Science.) University of Otago; 2016. http://hdl.handle.net/10523/6400.

104 Wright JJ, Sergejew.AA. Radial coherence, wave velocity and damping of electrocortical waves. Electroencephalography and Clinical Neurophysiology 1991; 79: 403-412.

105 Izhikevich EM, Desai NS. Relating STDP to BCM. Neural Computation 2003; 15: 1511-1523.

106 Tang J, Maximov A, Shin O-H, Dai H, Rizo J, Sudhof TC. A complex/synaptotagmin 1 switch controls fast synaptic vesicle exocytosis. Cell 2006; 126: 1175-1187. doi:10.1016/j.cell.2006.08.030.

107 Henson SM, Cushing JM. Heirarchical models of intra-specific competition: scramble versus contest. Journal of Mathematical Biology 1996; 34: 755-772.

108 Friston K. Transients, metastability, and neuronal dynamics. Neuroimage 1997; 5: 164-171. doi: 10/1006/nimg.1997.0259.

109 Bellman, R. Adaptive Control Processes: a Guided Tour. Princeton University Press; 1961.

110 Cohen R, Havlin S. Scale- free networks are ultra-small. Physical Review Letters 2003; 90:058701. doi: 10.1103/ PhysRevLett.90.058701.

111 Sholl DA. The Organization of the Cerebral Cortex. Wiley, New York; 1956.

112 Stuart G, Spruston N, Sakmann B, Hausser M. Action potential initiation and backpropagation in neurons of the mammalian CNS. Trends Neuroscience 1997;. 20: 125-131.

113 Wright JJ, Bourke PD. On the dynamics of cortical development: synchrony and synaptic self-organization. Frontiers in Computational Neuroscience 2013; doi: 10.3389/fncom.2013.00004.

114 Wright JJ, Bourke PD. Further work on the shaping of cortical development and function by synchrony and metabolic competition. Frontiers in Computational Neuroscience 2016; doi: 10.3389/fncom.2016.00127.

115 Jarzynsky C. Nonequilibrium equality of free energy differences. Phys. Rev. Lett 1997; 78: 2690 – 2693. doi.org/10.1103/PhysRevLett.78.2690.

116 Prigogine I. Time, Structure, and Fluctuations. Science 1978 ; 201, 777-785.

117 MacLean PD. The Triune Brain in Evolution: role in paleocerebral functions. Plenum Press: New York; 1990.

118 Olds J, Milner P. Positive reinforcement produced by stimulation of septal area and other regions of rat brain, Journal of Comparative Physiological Psychology 1954; 47: 419–427.

119 Holroyd CB, Coles GH. The neural basis of human error processing: reinforcement learning, dopamine and the error-related negativity. Psychological Review 2002; 109: 679 – 709. doi: 10.1037//0033-295X.109.4.679.

120 Pawlak V, Wickens JR, Kirkwood A, Kerr JND. Timing is not everything: neuromodulation opens the STDP gate. Frontiers in Synaptic Neuroscience 2010; doi:10.3389/fnsyn.2010.00146.

121 Friston K, Ao P. Free energy, value and attractors, Computational and Mathematical Methods in Medicine 2012; doi.org/10.1155/2012/937860.

122 Wright JJ. Unilateral Pleasure-centre Stimulation in Split-Brain cats. Experimental Neurology 1973; 70: 278-285.

123 De Schutter E. Why are computational neuroscience and systems biology so separate? PLoS Computational Biology 2008; 4:e1000078. doi.org/10.1371/pcbi.1000078.

124 Amit DJ. Modelling Brain Function. Cambridge University Press; 1989.

125 Rosenblatt F. The perceptron: a probabilistic model for information storage and organization in the brain. Psychological Review 1958; 65: 386-408.

126 Sabour S, Frosst N, Hinton GE. Dynamic routing between capsules. 31st Conference on Neural Information Processing Systems (NIPS 2017) Long Beach, California. arXiv:1710.09829v2 [cs.CV];2017.

127 Rumelhart DE, Hinton GE, Williams RJ. Learning representations by back-propagating errors. Nature 1986; 323: 533-536.

128 Wright JJ, Bourke PD, Favorov OV. Mobius-strip-like columnar functional connections are revealed in somato-sensory receptive field centroids. Frontiers in Neuroanatomy 2014; doi: 10.3389/fnana.2014.00119.

129 Markram H, Lübke J, Frotscher M, Sakmann B. Regulation of synaptic efficacy by coincidence of postsynaptic APs and EPSPs. Science 1997; 275: 213–215. doi:10.1126/science.275.5297.213.

130 Bienenstock EL, Cooper LN, Munro PW. Theory for the development of neuron selectivity: orientation specificity and binocular interaction in visual cortex. Journal of Neuroscience 1982; 2: 32–48.

Declaration of interests

☒ The authors declare that they have no known competing financial interests or personal relationships that could have appeared to influence the work reported in this paper.

☐The authors declare the following financial interests/personal relationships which may be considered as potential competing interests:

The authors declare that they have no known competing financial interests or personal relationships that could have appeared to influence the work reported in this paper.